

A Theoretical Lunar Ionosphere

HERSCHEL WEIL AND MURRAY L. BARASCH

Radio Astronomy Observatory, University of Michigan, Ann Arbor, Michigan

Communicated by Sydney Chapman

Received October 23, 1962

The consequences of a mechanism originally used by Herring and Licht for computing a possible lunar ionosphere are investigated in more detail than was done by these authors. The mechanism assumes that protons of the solar flux which strike the moon are re-emitted as hydrogen atoms, some of which are reconverted to protons by charge exchange. There results a single layer ionosphere. In this paper simplifying assumptions made by Herring and Licht of complete spherical symmetry and an everywhere constant mean radial velocity for the emitted atoms are removed. Quite different procedures are then necessary and the effects of an incident flux coming from only one direction are brought out. For typical quiet sun solar stream parameters the resulting ionosphere has a single layer with a maximum electron number density of roughly 350 cm^{-3} at 0.6 lunar radii above the lunar surface on the moon-sun connecting line. There is only slow variation with angle of the radial location and magnitude of the maximum of the layer until about 60° off this direction; then rapid decreases in both location and magnitude begin. During times of enhanced solar activity the ionosphere according to this model would increase. However, the theory will likely not hold during storms associated with solar magnetic tongues.

INTRODUCTION

The few experimental and theoretical studies to date which have concerned themselves with determining the extent and magnitude of a lunar ionosphere indicate that a tenuous one exists with a maximum number density of the order of 10^4 cm^{-3} corresponding to a plasma frequency of about one Mc/s. From the point of view of the radio astronomer, this suggests that the moon would be an ideal place to locate radio receivers for monitoring low frequency galactic and solar emissions which do not penetrate the terrestrial ionosphere and also to provide an earth-moon base line for simultaneous higher frequency measurements of solar bursts. Once established with suitable communication links to the earth, such receivers would possess considerable operational advantages over

receivers carried for the same purpose on man-made satellites.

Experimental evidence for a lunar ionosphere by rough but direct measurements was furnished by Gringauz *et al.* (1961) by particle counters on Lunik III which found an increase in electron density above ambient beginning at about 10 moon radii. Indirect experimental evidence yielding bounds on the possible electron content of a lunar ionosphere was presented by Elsmore (1957) who interpreted the duration observed at 3.7 meter wavelength of an occultation of radiation from the Crab nebula by the moon as being due to direct shadowing by the moon itself plus an outward refractive bending of the paths of the radio waves by a lunar ionosphere. Assuming a negative exponential variation of electron number density with height for the

ionosphere, he was led to conclude that the maximum density was of the order of 10^3 cm^{-3} assuming a scale height of 20–80 km, or $10^3 \text{ cm}^{-3} \leq n_e \leq 10^4 \text{ cm}^{-3}$ for scale heights of 80–5000 km. The experimental accuracy of the basic observations was, however, marginal.

Herring and Licht (1960) have put forth a theory of the formation of a lunar ionosphere. They consider a solar wind composed of protons and electrons incident on the moon and re-emission of the solar protons incident on the lunar surface as a gas of neutral hydrogen atoms at the temperature of the moon's surface.¹ By charge exchange ($\text{H} + p \rightarrow p + \text{H}$) with the further incoming high-speed solar protons a lower speed set of protons is developed. These, together with the electrons which originally neutralized the solar stream macroscopically, now form an ionospheric component in addition to the incident solar stream itself. A comparison of the charge exchange rate with that for photoionization is given by Herring and Licht which shows that charge exchange is the dominant of these two processes. In Appendix A we compare the rate for the above charge exchange process with various competing processes and with recombination. Herring and Licht carried out admittedly crude computations according to this basic idea to obtain curves of electron density versus radial distance from the moon's center. They were led to results in apparent accord with Lunik data quoted above, reaching a peak of 400 cm^{-3} at about 2 lunar radii.

In discussing his results Elsmore considered briefly the possibility of formation of an ionosphere exceeding the ambient by reemission of solar wind particles. He also assumed neutralization of the incoming particles, but did not consider the possibility of charge exchange. Hence he ruled out this source of an ionosphere.

The work to be described in this paper is essentially a more careful application of

¹ A theoretical investigation supporting this neutralization and thermalization for protons which strike the moon has since been reported in a talk by Gold (1962).

the mechanism suggested by Herring and Licht. This has led to somewhat different values for the location and magnitude of the ionization maximum and also to a determination of the variation of n_e with angle away from the subsolar point. Angular variation is not obtainable from the treatment by Herring and Licht.

PROCEDURE AND RESULTS

To investigate the ionosphere formed by the above mechanism requires solving two partly coupled continuity equations for n_p , the density of low temperature protons resulting from charge exchange with H atoms of density n_H . Since recombination can be neglected (see Appendix A) these equations are just

$$\text{div } n_H \bar{v} = -J\sigma n_H, \quad (1)$$

$$\text{div } n_p \bar{v} = J\sigma n_H \quad (2)$$

where σ is the charge-exchange cross section, J the solar proton flux, and \bar{v} the local velocity of the slow particles. In order to solve these equations to obtain a first approximation to the ionosphere formed by this mechanism Herring and Licht neglected gravitational and magnetic field effects and assumed a constant \bar{v} directed radially outward. However, even if gravity and magnetic field effects are to be ignored this assumption on velocity is poor, in that it is not in accord with the idea of diffuse reflection from the moon which would be consistent with the assumed thermalization of the emitted particles. It also in effect assumes that the incident solar stream is directed radially inward as though from a spherical source concentric with the moon.

This velocity assumption may be removed by procedures which are outlined here, the details constituting Appendix B. Gravitational and magnetic field effects will still be ignored in this procedure although modifications to the results which gravitational effects would bring about are discussed *a posteriori*. Magnetic field effects will also be considered, leading to a probable limitation of the present analysis to exclude periods of solar-flare-associated enhancement of the solar wind. A velocity

\bar{v} to insert in the equations was computed by first integrating the collision-free Boltzmann equation, taking into account the spherical perturbing moon surface. In this

for a scale factor, was already available in Dolph and Weil, 1961.)

The n_H used is then accurate for slow neutrals up to the error introduced by neg-

TABLE I
SOLAR STREAM DATA

	Chamberlain (1961)	Parker (1961a)	Herring and Licht (1960)	Noise storms max Parker (1961a)
Velocity (km/sec) V	18	400	10^3	10^3
Temperature ($^{\circ}\text{K}$)	15000-20000	700	Not specified	Not specified
Number density, (cm^{-3}) of protons, n_p	30	200	Not specified	10^5
Flux of protons ($\text{cm}^{-2} \text{sec}^{-1}$)	12×10^{7a}	8×10^9	10^{10}	10^{13}
Charge-exchange cross section (cm^2)	4.5×10^{-15}	2.2×10^{-15}	10^{-15}	—

^a Allowing for the fact that the moon's velocity of 30 km/sec perpendicular to the moon-sun ray becomes appreciable for so slow a solar stream velocity as 18 km/sec.

the procedure of Wang Chang (1950) modified to allow for the thermalization at the lunar surface temperature was followed. The resulting distribution function, multiplied by velocity, was then integrated over

lecting slow neutrals lost during charge exchange. The smallness of the product of solar flux times σ makes this error negligible.

The n_H and \bar{v} functions thus obtained were substituted into Eq. (2). The result-

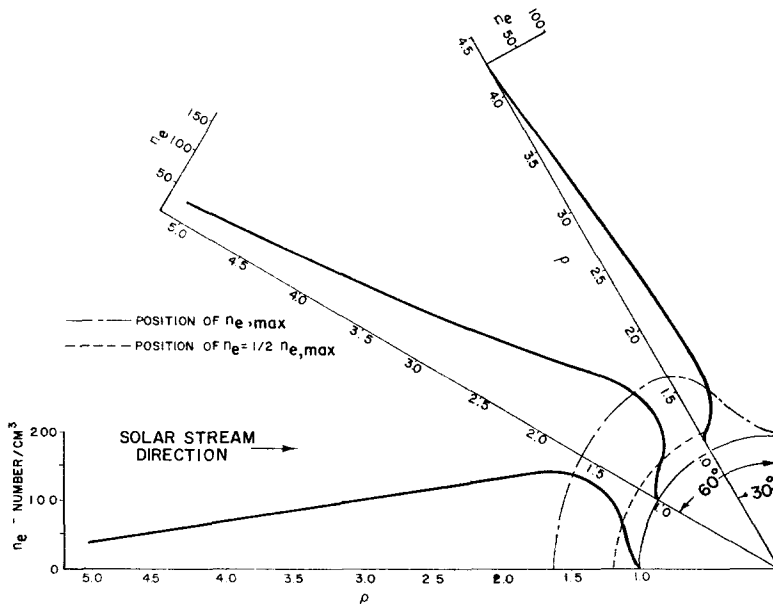


FIG. 1. Electron density associated with protons formed by charge exchange [solutions of Eq. (2)].

velocity space to yield an average velocity vector \bar{v} as a function of position. Likewise, n_H determined by integrating the distribution function itself over velocity space rather than by solving Eq. (1) was used in Eq. (2). (This result for n_H , except

ing equation was integrated numerically along radials from the moon's center using a desk calculator. Basic solar flux estimates due to Parker (1961a) and a charge exchange cross section due to Fite *et al.* (1958), as given in the second column of

Table I, were used. The value of n_p was taken as zero at the lunar surface since three-body recombination should proceed rapidly enough within the subsurface region where thermalization occurs so that

is along the moon-sun connecting line. In addition to these curves similar curves were computed at 88° and 88.5° , but the peaks occur so close to the lunar surface and of such small magnitude that they cannot be shown on the same scale as Fig. 1. They were used, however, to draw Fig. 2 and the curve of the location of maximum

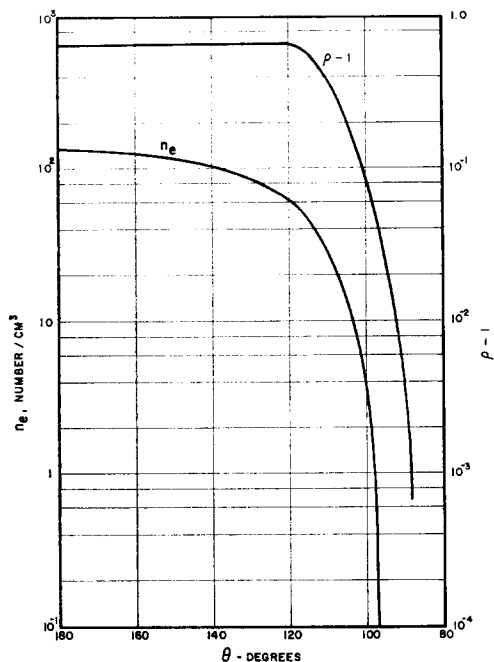


FIG. 2. Value and radial location of maximum electron density due to charge exchange as a function of angle.

no slow protons formed there by charge exchange are re-emitted as protons. The ionosphere computed by this procedure is illustrated in Figs. 1-4. In Fig. 1 are shown the n_e values computed along three radial lines as functions of ρ . The $\theta = 180^\circ$ radial

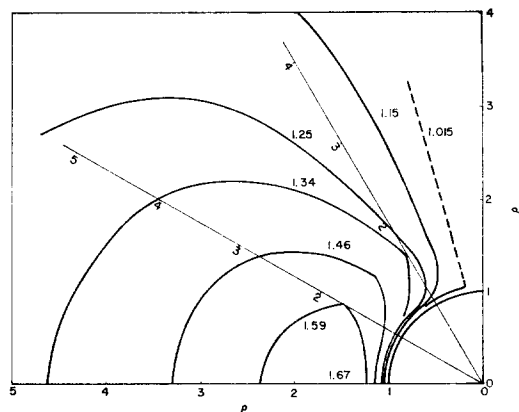


FIG. 3. Equidensity contours on the irradiated side of the moon.

n_e on Fig. 1, which illustrate the very rapid rate at which both the location and magnitude of the peak n_e decrease beyond about 60° from the moon-sun connecting line. In fact there is effectively no ionosphere produced by this mechanism beyond about 80° from this line. Both maximum n_e and its radial distance are less than the values found by Herring and Licht, who obtained $n_e \text{ max} = 400 \text{ cm}^{-3}$ at two lunar radii.

The moon shadows the incoming stream and its effect is felt even slightly ahead of

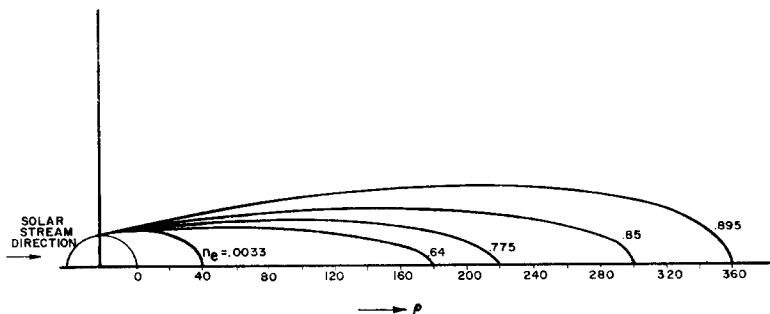


FIG. 4. Approximate equidensity contours of n_e behind the moon due to shadowing of solar flux. (The intercepts with the sphere and axis are computed points.)

the moon by virtue of the moon's blocking of the relatively few particles which would be traveling in the general direction of the sun against the over-all streaming motion. These shadowing effects were investigated by Dolph and Weil (1961) and the formulas are in Appendix B, Eqs. (B 10) and (B 11). For the numerical data being used there is essentially no effect ahead of the moon and the n_e due to the incident stream may be taken to be constant; for this computation, 200 cm^{-3} . Behind the moon there is a very extended shadow region. The values of n_e along the back surface of the moon and along the symmetry line $\theta = 0$ at the rear were computed from Eqs. (B 10) and (B 11). Computation of n_e at off axis points involves extensive numerical work and so was not carried out. Using only two computed points per curve (one on the sphere, one on the axis) equidensity curves of n_e behind the moon are presented in Fig. 4. The shape of similar curves computed and drawn in detail (but for quite different parameter values) by Dolph and Weil (1961) was used as a guide to estimating the general shape of the curves. Finally equidensity curves of n_e ahead of the moon are given in Fig. 3. These are based on the same data as Figs. 1 and 2 but include also the incident stream electron density.

For larger n_p or V of the incident stream the effect will be to scale the magnitude of the peak n_e proportionally, while greater temperature T_1 for the incoming stream will scale the peak n_e proportional to $\sqrt{T_1}$.

GRAVITATIONAL EFFECTS

The effect of the lunar gravitational field on the particle trajectories has been neglected. This means really that three different effects which would modify the results have been omitted. One effect is the curvature of the trajectories of the incoming solar particles so as to increase the incident flux, particularly near the limb. The second effect is the curvature of the hydrogen atom trajectories during the outward flight of the atoms. This affects both the orbit geometry and the time available for charge

exchange. The third effect is the availability for charge exchange, during their return from apogee, of the atoms which do not escape the moon's gravitational field.

At the assumed lunar surface temperature of 315°K , 95% of the emitted particles reach an altitude of 2.5 moon radii against gravity, well past the computed distance of about 1.6 moon radii for maximum n_e , and, in fact, about 50% of the atoms escape. The first two effects will therefore serve primarily only to increase n_p somewhat near the limbs where the primary effect yields at best only a very small n_p of little practical interest.

The third effect concerning incoming atoms will apply to roughly one-half the atoms. Along any radial line there will be contributions to n_e from some of these incoming particles. These start from rest from locations governed by a rather wide distribution function, quite unlike the ordered starting condition at $r = R$ for the outgoing particles. Hence one would expect their contribution to n_p to possess no well-defined maximum as does the contribution of the outgoing particles. Thus the general shape of the computed curves can be expected to hold without gross distortion although the over-all ionization level will be somewhat increased. To actually check this expectation by a more exact analysis taking gravity into account is a fairly complex task. For example, the following procedure reminiscent of that used by Opik and Singer (1959) to determine exospheric density distributions could be applied to handle gravitational effects on the emitted atom distribution for a uniform stream incident from one direction.

The contribution of each atom to its relative density $n(p)$ will be proportional to its transit time τ across the curvilinear rectangle of sides $r d\theta$ and dr located at $P(r, \theta_1)$. If the atom's radial velocity v_r exceeds its tangential velocity v_t at P then $\tau \propto [v_r(P)]^{-1}$, otherwise $\tau \propto [v_t(P)]^{-1}$. These velocities may be associated with the initial radial and tangential velocity components v_{0r} and v_{0t} at $r = R$ by invoking conservation of angular momentum and of energy. Thus one can find n_H by multiplying the

initial distribution of atoms by their probability distribution for velocities [Eqs. (B 1) and (B 6)] and integrating as follows:

$$n_H(r, \theta_1) = \int_{v_0 > v_{min}} dv_0 \int_{\Theta_1(v_0)} \frac{f_2(\bar{v}_0, R, \theta_0)}{v_r(r, v_0, \theta_0)} d\theta_0 \\ + \int_{v_0 > v_{min}} dv_0 \int_{\Theta_2(v_0)} \frac{f_2(\bar{v}_0, R, \theta_0)}{v_t(r, v_0, \theta_0)} d\theta_0.$$

The lower limit v_{min} is the initial velocity which will enable an atom ejected radially to just reach radius r . Thus

$$\frac{1}{2}mv_{min}^2 = k/r.$$

The θ_0 ranges $\Theta_1(v)$ and $\Theta_2(v)$ are to be determined as follows: $\Theta_1(v_0)$ includes all θ which for a given v_0 lead to $v_r(P) > v_t(P)$; $\Theta_2(v_0)$ includes all θ which for a given v_0 lead to $v_t(P) > v_r(P)$. This formulation is amenable to evaluation on an electronic computer.

MAGNETIC EFFECTS

Effects due to possible magnetic field in the vicinity of the moon are difficult to take into account partly because of lack of knowledge of the field's structure and magnitude. The best experimental data is probably Lunik II data reported by Gringauz *et al.* (1961) and elsewhere, which simply indicated that the magnetic field measured near the moon was not greater than 100γ . This is much less than the 260γ field which would yield a magnetic pressure equal to the pressure or kinetic energy density in the incoming stream for the Parker quiet sun data in Table I.

If the moon's possible self-field is neglected the magnetic field near the moon is due only to magnetic field carried along with the solar particles. In this case the field structure depends greatly on the form of the incident field (which is at present a subject of extensive investigation) and on the conductivity of the moon. Recall from magnetohydrodynamics theory that within a stationary medium of conductivity σ the magnetic field is governed by the diffusion equation so that a given magnetic field configuration of characteristic length L will

decay exponentially to e^{-1} of its original value in a time

$$\tau = 4\pi\sigma L^2/c^2 \text{ (Gaussian units).}$$

Therefore τ is a rough measure of the time for a magnetic field line to diffuse a transverse length L .

To estimate τ for the moon requires use of some mean value of σ . One has only estimates of the values of σ near the lunar surface. The deepest probe, radar, has yielded a value for σ of about $3 \times 10^6 \text{ sec}^{-1}$ (Senior and Siegel, 1960). This corresponds to τ equal to 1260 sec, or 21 minutes, for L equal to a lunar radius.

To be consistent with the Parker picture of a solar stream from the quiet sun the magnetic field is expected to be primarily directed along the flow direction of the incident stream (Parker, 1961b). This is in accord with Explorer X data given by Heppner *et al.* (1962). When a magnetic field so oriented is initially incident on the moon, it will at first follow the flow lines around the moon but it will diffuse inward so that, after a few τ , a steady state field showing essentially no perturbation will prevail; the field lines will continue through the moon. This result will hold even if the moon has a high conductivity core, since the field will simply diffuse into the low σ lunar surface layer in some fraction of the $\tau \sim 21$ minutes diffusion time. The protons will spiral in about these field lines with a radius of gyration of about 10^{-3} lunar radii as determined by the unperturbed field strength of two gamma and the mean thermal speed. In this situation, one would therefore not expect great modification of the present analytical results which ignored magnetic fields. The same situation may also be expected during solar wind enhancements due to M region storms.

Solar flares, however, change the incident magnetic field so that it may be primarily transverse to the direction of the incidence of the solar stream in accord either with mechanisms given by Gold (1961) or by Parker (1961b). In this case the lunar diffusion time of 21 minutes must be compared with the transit time of a few seconds for a solar stream particle to trav-

erse a lunar diameter. Thus the transverse field line moving along with incoming stream will have no time to diffuse far into the moon and will be drawn around it by the stream. Then, as Gold (1962) has suggested, the magnetic field lines on the irradiated side of the moon will be compressed until the magnetic and kinetic pressures become equal and the field lines will be carried around the moon, drawing together again well behind the moon. In this case a fraction of the incident protons spiralling around the field lines in the intensified field ahead of the moon will never strike the lunar surface and for these the ionosphere forming mechanism considered in the paper cannot apply. This fraction will in fact constitute the major part of the particles if the mean radius of gyration of the protons in this enhanced field is less than the distance from the lunar surface at which magnetic and kinetic pressure are equal.

ACKNOWLEDGMENTS

The authors would like to thank Professor Fred T. Haddock for pointing out the interest in a study of a possible lunar ionosphere being generated by the solar flux and to acknowledge his and J. M. Malville's most useful discussion and criticism. They would also like to acknowledge the careful calculating of the solutions of Eq. (2) by Harold E. Hunter. This work was supported by the National Aeronautics and Space Administration, Contract NsG 181-61.

APPENDIX A

Rates of Competing Processes

This theory of the lunar ionosphere is based on the concept that protons of the solar wind are re-emitted as neutral H atoms after striking the lunar surface. By charge exchange with the incident protons, the H atoms are then converted to slow protons. These slow protons together with the electrons which originally balanced the charge of those fast protons that took part in the charge exchange, form an augmentation of the lunar ionosphere above the solar wind level.

In order for this to be valid, once the assumption of ejection of H atoms is made,

the rates of competing extraneous processes must be shown to be negligible. In particular, radiative association to form H₂ and photoionization of H must be shown unimportant compared to charge transfer. We shall now investigate this.

First, since charge transfer between H₂ and H⁺ is quite inefficient, it is necessary to assure ourselves that the re-emitted H atoms remain atomic. For this purpose, we refer to the estimate by Chamberlain (1961) that the rate coefficient for radiative association is at best $\alpha = 10^{-15}$ cm³/sec, and not very temperature sensitive. This coefficient α is to be inserted into the usual bimolecular decay law $dn_H/dt = -\alpha n_H^2/\text{cm}^3 \text{ sec}$ and the rate compared to the charge transfer rate.

Next, to be sure that photoionization is not more important than charge transfer in creating an ionosphere, we use the result given by Hinterregger (1961) that the integral of the product of solar flux and photoionization cross section for H at the top of the earth's atmosphere is roughly 5×10^{-7} /sec atom. The photoionization rate is thus

$$dn_H/dt \sim 5 \times 10^{-7} n_H \text{ cm}^{-3} \text{ sec}^{-1}.$$

The charge transfer rate is given by $dn_H/dt = -n_p v_{\text{rel}} \sigma n_H \text{ cm}^{-3} \text{ sec}^{-1}$, where $n_p v_{\text{rel}}$ is the solar proton flux, relative to the slow H gas, and σ is the charge transfer cross section, which may be obtained from Fite *et al.* (1958) as given in Table I.

We will evaluate the ratios of rates for these processes for two sets of parameters, which arise from theories of Parker (1961a) and (Chamberlain (1961), respectively, describing the solar wind for quiet-sun conditions. These lead to values for the density of the slow "rebound" hydrogen atoms which for the Parker parameters are given in Table II.

On the axis, for $r/R = 1$, $n_H/n_p = 0.55$ from the Chamberlain parameters. The rates for the charge transfer and photoionization are in the ratio

$$\frac{n_p v_{\text{rel}} \sigma}{5 \times 10^{-7}} \gtrsim 35$$

for the Parker parameters, so that we may safely neglect photoionization as a mechanism for generating an ionosphere in that

case. For Chamberlain's values, the relative velocity should really include the effect of the moon's orbital velocity around the sun of roughly 30 km/sec, giving a net value of $\sqrt{18^2 + 30^2}$, or about 35 km/sec, and we find that the rates of photoionization and charge transfer are approximately equal. Thus, neglect of photoionization in this case

ionosphere. This may be bounded by putting $n_{p_2} = n_H$, an extreme assumption of 100% ionization. The bound for the Parker theory is of the order of 30, and for the Chamberlain theory also. Thus, the ionospheric density seems to be controlled by convection rather than recombination, and the continuity equation may be written neglecting recombination.

TABLE II

	r/R	n_H/n_{p1}
On axis of incident wind direction	1	300
	1.5	120
	2	60
	4	35
35 degrees off axis	1	250
70 degrees off axis	1	100
90 degrees off axis	1	15

would cause a 50% error in the production rate of ions. It could be taken care of by an adjustment of the right-hand side of Eq. (2) and would scale the results without distorting the shape of the n_e vs. r curves.

As for the radiative association, the ratio of the charge transfer rate to the rate for this process is

$$\frac{n_{p_1} v_{rel} \sigma n_H}{10^{-15} n_H^2} \sim 10^5 \text{ to } 10^6$$

for Parker's model and also for Chamberlain's. It is clearly justified to assume that the atomic hydrogen does not become molecular.

Another point to be investigated is whether the neglect of recombination with respect to production rate in the equation of continuity (which is used to determine the slow proton density) is justified. The recombination rate coefficient is given by Field (1960) as $(4 \times 10^{-9}/T)$ cm³/sec/°K where T is the temperature of the slow protons, which we take as the lunar surface temperature, 315°. The ratio of the production to recombination terms is then

$$\frac{n_{p_1} v_{rel} \sigma n_H}{10^{-15} n_{p_2}^2}$$

where n_{p_1} is the density of incident fast protons and n_{p_2} that of slow ones composing the

APPENDIX B

Perturbations of Dilute Corpuscular Streams

The distribution, n , of heavy particles is made up of two contributions, n_1 the number density of main stream protons which have not been in contact with the sphere and $n_2 \equiv n_H$ the number density of reflected or re-emitted particles which we will take to be neutrals. The densities n_1 and n_2 are integrals over all speeds and all possible directions of particle motion (taking into account the shadowing by the sphere) of the corresponding velocity distribution functions f_1 and f_2 . If, at the surface, the temperature, T_2 , of the gas of re-emitted particles is less than T_1 the flux of emitted particles must be greater than it is in the equal temperature case at equilibrium to maintain equality of the incoming and outgoing fluxes. This flux equality is used by Herring and Licht (but without a temperature scaling factor) to determine the lunar atmosphere. The scale factor will simply be the ratio of mean or most probably velocities corresponding to T_2 and T_1 , hence it is $\sqrt{T_1/T_2}$.² We show this formally below, but for the moment note that this factor is applied only to n_2 and not to n_1 . However, near the sphere, n_2 , which represents a "snow-plowing effect," is predominant so that effectively the entire density is scaled. On the other hand, far from the

² These remarks assume a uniform surface temperature of the moon for which has been used the mean temperature measured between the subsolar point and the limb; i.e., $T_2 = 315^\circ\text{K}$. For the low velocity Chamberlain case where the effective direction of the wind is at a large angle from the moon-sun connecting line the appropriate mean temperature would be lower. It should be pointed out that this would make the modifications to the present solution due to gravitational effects more severe.

sphere, n_2 becomes negligible and there is no scaling.

For a more detailed picture, we shall assume isotropic emission or reflection from the sphere surface and use the symbol \bar{V} for the streaming velocity. Then, following Wang Chang (1950) the velocity distribution for re-emitted particles at the sphere surface is written with a space-dependent factor A , to be determined, as

$$f_2(c) = An_0(2kT_2/\pi m)^{-3/2} \exp [(-m/2kT_2)c^2] S(\hat{\mathbf{c}}) \quad (\text{B1})$$

where $S = 1$ for \mathbf{c} directed out of the sphere and $S = 0$ for other \mathbf{c} . Directly on the sphere A is a function only of $\hat{\mathbf{n}}$, the unit normal to the surface at the point of interest. The incident stream has distribution

$$f_1(\mathbf{c}; V) = n_0(2kT_1/\pi m)^{-3/2} \exp [(-m/2kT_1)(\mathbf{c} - \mathbf{V})^2] (1 - S). \quad (\text{B2})$$

In these formulas, k is a Boltzmann's constant, m is proton mass, and \mathbf{c} particle velocity; n_0 is number density of the unperturbed stream, and T_1 and T_2 are temperatures of the stream and the moon, respectively.

At the surface the constant A is to be determined by the flux continuity requirement so that, with $\hat{\mathbf{n}}$ representing the outward unit normal to the sphere,

$$\begin{aligned} & \int \int \int d\mathbf{c} \hat{\mathbf{n}} \cdot \mathbf{c} (1 - \text{sign } \hat{\mathbf{n}} \cdot \hat{\mathbf{c}}) f_1(\mathbf{c}; \mathbf{V}) \\ &= -A \int \int \int d\mathbf{c} \hat{\mathbf{n}} \cdot \mathbf{c} (1 + \text{sign } \hat{\mathbf{n}} \cdot \hat{\mathbf{c}}) f_2(\mathbf{c}), \end{aligned} \quad (\text{B3})$$

where $\text{sign } \hat{\mathbf{n}} \cdot \hat{\mathbf{c}} = \hat{\mathbf{n}} \cdot \mathbf{c} / |\hat{\mathbf{n}} \cdot \mathbf{c}|$. In the left-hand integral change to dimensionless variables

$$\bar{\mathbf{V}}' = \bar{V} / \sqrt{2kT_1/m}, \quad \mathbf{c}' = \mathbf{c} / \sqrt{2kT_1/m}. \quad (\text{B4})$$

In the right-hand integral change to

$$\mathbf{c}'' = \mathbf{c} / \sqrt{2kT_2/m}.$$

Then, dropping the primes in the integrands of the definite integrals, one has

$$\begin{aligned} & \sqrt{T_1/T_2} \int \int \int d\mathbf{c} \hat{\mathbf{n}} \cdot \mathbf{c} (1 - \text{sign } \hat{\mathbf{n}} \cdot \mathbf{c}) \\ & \quad \exp [-(\mathbf{c} - \mathbf{V}')^2] \\ &= A \int \int \int d\mathbf{c} \hat{\mathbf{n}} \cdot \mathbf{c} (1 + \text{sign } \hat{\mathbf{n}} \cdot \mathbf{c}) \\ & \quad \exp (-c^2). \end{aligned} \quad (\text{B5})$$

This is identical with the equation used by Wang Chang except for the factor $\sqrt{T_1/T_2}$ which enters formally because of the necessity to normalize the \bar{c} factor differently on each side. $A(\hat{\mathbf{n}}')$ is obtained by replacing \bar{n} by $\hat{\mathbf{n}}'$ in the expression for $A(\hat{\mathbf{n}})$ after integration and is

$$A(\hat{\mathbf{n}}') = \{ \exp -[(\mathbf{V}' \cdot \hat{\mathbf{n}}')^2] - \sqrt{\pi} \mathbf{V}' \cdot \hat{\mathbf{n}}' \text{erfc}(\mathbf{V}' \cdot \hat{\mathbf{n}}') \} \sqrt{(T_1/T_2)}. \quad (\text{B6})$$

Thus $A(\hat{\mathbf{n}})$ and its generalization to its functional form for points off the sphere, $A(\hat{\mathbf{n}}')$ are simply scaled by $\sqrt{T_1/T_2}$ from Wang Chang's.

The scale factor then carries over to n_2 , which is found by integration of f_2 in velocity space. The integrations are carried out in Dolph and Weil (1961) and lead to the approximate formula³

$$\begin{aligned} n_2(r, \theta) &= (n_0/2) \sqrt{(T_1/T_2)} \{ (1 - P) \\ & \quad \exp(-V'^2 \rho^2 \cos^2 \theta_0) \\ & \quad - \sqrt{\pi} V' \rho \cos \theta_0 \text{erfc}(V' \rho \cos \theta_0) \\ & \quad [1 - P - \frac{1}{3}(1 - P^3) + (1/3)\rho^3] \} \end{aligned} \quad (\text{B7})$$

wherein $\rho = r/R$ is the ratio of distance from the sphere center to sphere radius, $P = \sqrt{1 - (R^2/r^2)}$ and θ_0 is the polar angle measured from the direction of \mathbf{V} about the sphere center. Thus $\theta_0 = \pi$ represents the symmetry axis on the side of the sphere which faces the incoming particle stream. In particular on the surface

$$\begin{aligned} n_2(R, \theta_0) &= (n_0/2) \sqrt{(T_1/T_2)} \{ \exp(-V'^2 \cos^2 \theta_0) \\ & \quad - \sqrt{\pi} V' \cos \theta_0 \text{erfc}(V' \cos \theta_0) \}. \end{aligned} \quad (\text{B8})$$

³ In Dolph and Weil's paper this expression is given in terms of an integral I_3 printed with a 2π factor which should be unity. The correct formula was used in their computations.

Furthermore,

$$n_1 = (n_0/2) \{1 + 2 \exp(-V'^2 \sin^2 \theta_0) \int_0^\infty duu \exp(-u^2) \operatorname{erf}(u\rho^2 P - V' \cos \theta_0) I_0(2uV' \sin \theta_0)\} \quad (\text{B9})$$

where I_0 is a Bessel function of imaginary argument. An exact evaluation of the integral is possible for $\theta_0 = 0$, $\theta_0 = \pi$ for all r , and for all θ_0 when $r = R$.

For $r = R$,

$$n_1(R, \theta_0) = (n_0/2) \operatorname{erfc}(V' \cos \theta_0). \quad (\text{B10})$$

For $\theta_0 = 0$

$$n_1(r, \theta_0) = (n_0/2) \{ \operatorname{erfc}(V') + P \exp[-(V'/\rho)^2] \operatorname{erfc}(-V'P) \} \quad (\text{B11})$$

For $\theta_0 = \pi$,

$$n_1(r, \pi) = (n_0/2) \{ \operatorname{erfc}(-V') + P \exp[-(V'/\rho)^2] \operatorname{erfc}(V'P) \} \sim n_0. \quad (\text{B12})$$

The last step is an approximation which is good when $V' \gtrsim 4$. In this case as $\exp(-V'^2 R^2/r^2)$ and P begin to become appreciable with increasing r , $\operatorname{erfc}(V'P)$ becomes essentially zero and the result $n_1 \sim n_0$ follows.

Thus we have $n_2(R, \theta_0)$ exceeding $\frac{1}{2}(1 + .9V')n_1$ even when $T_2 = T_1$. Thus along and near the sphere surface n_2 dominates and hence the scale factor $\sqrt{T_1/T_2}$ can reasonably be used for the entire distribution $n = n_1 + n_2$. For large r , this is not true and in this case $n_1 \rightarrow n_0$, $n_2 \rightarrow 0$ and there is of course no scaling. Figure 4 was obtained from $n_2(r, 0)/n_0$ and $n_2(R, \theta_0)/n_0$ computed for $V' = 120$ corresponding to the Parker numbers, and including the $\sqrt{T_1/T_2}$ factor which in this case is ~ 1.5 .

For the Chamberlain data of Table I, $V' \sim 1$ so that the distribution of n_2 will be almost independent of angle, but the scale factor $\sqrt{T_1/T_2} \sim 7$.

Using $f_2(c)$ as given by Eq. (B1) and (B6), the expression for \mathbf{v} is then

$$\mathbf{v} = \frac{n_0}{n_2 \pi^{3/2}} \int_0^\infty c^2 \exp(-c^2) dc \int_0^{2\pi} d\phi \int_0^{\theta_1} \sin \theta \{ \exp[-(\mathbf{V}' \cdot \hat{\mathbf{n}}')^2] - \sqrt{\pi} (\mathbf{V}' \cdot \hat{\mathbf{n}}') \operatorname{erfc}(\mathbf{V}' \cdot \hat{\mathbf{n}}') \} \mathbf{c} d\theta. \quad (\text{B13})$$

in terms of a polar coordinate system r, θ, ϕ centered at the moon's center and with \mathbf{r} as polar axis. The upper limit $\theta_1 = \cos^{-1} P$ so that $\sin \theta_1 = \rho^{-1}$. Here $\hat{\mathbf{n}}'$ is the unit normal to the sphere, so that

$$\mathbf{V}' \cdot \hat{\mathbf{n}}' = (V'r/R) \{ \cos \theta_0 - [\cos \theta - \sqrt{\cos^2 \theta - P^2}] [\cos \theta \cos \theta_0 + \sin \theta \sin \theta_0 \cos(\phi - \phi_0)] \}.$$

To evaluate the integral we follow Dolph and Weil in their determination of n_2 by neglecting the slowly varying function $\cos \theta - \sqrt{\cos^2 \theta - P^2}$ in the exponential $\exp[-(\mathbf{V}' \cdot \hat{\mathbf{n}}')^2]$ and integrating the resulting approximate integral for \bar{v} . Thus $\exp[-(\mathbf{V}' \cdot \hat{\mathbf{n}}')^2]$ is replaced by $\exp[-V'\rho \cos \theta_0]$, a constant during the integration.

Taking rectangular components in a system with $r = z$, we are led to the following three expressions for v_x, v_y , and v_z :

$$\begin{aligned} v_x &= (n_0 v' \rho / 2n_2) \operatorname{erfc}(V'\rho \cos \theta_0) \sin \theta_0 \cos \phi_0 \int_0^{\theta_1} \sin^3 \theta [\cos \theta - \sqrt{\cos^2 \theta - P^2}] d\theta, \\ v_y &= v_x \tan \phi_0, \\ v_z &= (2n_0/n_2 \sqrt{\pi}) \{ \exp[-(v'\rho \cos \theta_0)^2] \int_0^{\theta_1} \sin \theta \cos \theta d\theta + \sqrt{\pi} V'\rho \cos \theta_0 \\ &\quad [\int_0^{\theta_1} [\cos \theta - \sqrt{\cos^2 \theta - P^2}] \cos^2 \theta \sin \theta d\theta - \int_0^{\theta_1} \cos \theta \sin \theta d\theta] \} \end{aligned}$$

The integrals are all explicitly integrable. One obtains

$$v_x = (nV'/8n_2) \operatorname{erfc}(V'\rho \cos \theta_0) \sin \theta_0 \cos \phi_0 F_1(\rho)$$

where

$$F_1(\rho) = \frac{1}{\rho^3} - \left(1 + \frac{P^2}{2}\right) + P^2 \rho \left(1 + \frac{P^2}{4}\right) \log_e \left(\frac{\rho + 1}{\rho - 1}\right) \quad (\text{B14})$$

and

$$v_z = \frac{n_0}{2\sqrt{\pi n_2}} \left\{ \frac{1}{\rho^2} \exp[-(V'\rho \cos \theta_0)^2] - \frac{1}{2} \sqrt{\pi} V' \cos \theta_0 F_2(\rho) \operatorname{erfc}(V'\rho \cos \theta) \right\}$$

where

$$F_2(\rho) = \frac{1}{\rho^3} + 1 - \frac{P^2}{2} - \frac{\rho P^4}{4} \log_e \left(\frac{\rho + 1}{\rho - 1} \right).$$

These are the rectangular components of \bar{v} in a local system with $\hat{z} = \hat{r}$ at the observation point. In terms of coordinates in the spherical system about the wind axis ($v_r, v_{\theta_0}, v_{\phi_0}$):

$$\begin{aligned} v_r &= v_z, \\ v_{\theta_0} &= v_x \cos \phi_0 + v_y \sin \phi_0, \\ v_{\phi_0} &= -v_x \sin \phi_0 + v_y \cos \phi_0, \end{aligned}$$

and because of symmetry it suffices to solve Eq. (2) in the $\phi_0 = 0$ plane.

REFERENCES

- CHAMBERLAIN, JOSEPH (1961). Interplanetary gas III: A hydrodynamic model of the corona. *Astrophys. J.* **133**, 675-687.
- DOLPH, C. L., AND WEIL, H. (1961). On the change in radar cross section of a spherical satellite caused by a plasma sheath. In "Electromagnetic Effects of Re-Entry," pp. 123-132. Pergamon Press, London. See also: *J. Planet. and Space Sci.* **6**, 123-132.
- ELSMORE, B. (1957). Radio observations of the lunar atmosphere. *Phil. Mag., Ser. 8*, **2**, 1040-1046.
- FIELD, GEORGE (1960). The source of radiation from Jupiter at decimeter wavelengths, II. Cyclotron radiation by trapped electrons. *J. Geophys. Res.* **65**, 1661-1671.
- FITE, W. L., BRACKMAN, R. T., AND SNOW, W. A. (1958). Charge exchange in proton H-atom collisions. *Phys. Rev.* **112**, 1161-1169.
- GOLD, T. (1961). Present evidence concerning magnetic fields and particle fluxes in the solar system. In "Space Research II, Proc. Second International Space Science Symposium, Florence, 1961," pp. 803-812. North Holland Publishing Company, Amsterdam.
- GOLD, T. (1962). The hydrogen atmosphere of the moon. Presented at the Third International Space Science Symposium sponsored by COSPAR, Washington, D. C., May 8, 1962. Also: The Magnetosphere of the Moon. Presented at the Meeting of the American Astronomical Society, Yale University, New Haven, Conn., August, 1962.
- GRINGAUZ, K. I., BEZRUKIKH, V. V., OZEROV, V. D., AND RYBCHINSKII, R. E. (1961). A study of interplanetary ionized gas, energetic electrons and corpuscular solar emission, using three electrode charged particle traps set up on the second soviet cosmic rocket. In "Artificial Earth Satellites," pp. 122-129. Plenum Press, New York.
- HEPPNER, J. P., NESS, N. F., SKILLMAN, T. L., AND SCEARCE, C. S. (1962). Magnetic field measurements with the Explorer X satellite. *J. Phys. Soc. Japan* **17**, Supplement A-II, International Conf. on Cosmic Rays and the Earth Storm, Pt. II, 546-552 and 560.
- HERRING, J. R., AND LIGHT, A. L. (1960). The effect of solar wind on the lunar atmosphere. In "Space Research I, Proc. First International Space Science Symposium, Nice, 1960," pp. 1132-1145. North Holland Publishing Company, Amsterdam.
- HINTEREGGER, H. E. (1961). Telemetering monochromator measurements of extreme ultraviolet radiation. In "Space Astrophysics" (William Liller, ed.). McGraw-Hill, New York.
- OPIK, E. J., AND SINGER, S. F. (1959). Distribution of density in a planetary exosphere. *Phys. Fluids* **2**, 653-655. This paper contains the derivation which suggested the present treatment. Consequences of this paper, a correction, and a critique of related work are given in Part II. *Phys. Fluids* **4**, 221-233 (February, 1961).
- PARKER, E. N. (1961a). The solar wind. In "Space Astrophysics" (William Liller, ed.). McGraw-Hill, New York. See p. 163 and Eq. (9), p. 161.
- PARKER, E. N. (1961b). The solar wind. *J. Res. Nat. Bur. Stds.* **65D**, 537-542.
- SEGEL, K. M., AND SENIOR, T. B. A. (1960). A theory of radar scattering by the moon. *J. Res. Nat. Bur. Stds.* **64D**, 217-229.
- WANG CHANG, C. S. (1950). Transport phenomena in very dilute gases, II. *Eng. Res. Inst. EM-654*, University of Michigan, Ann Arbor.